

Modelling the seismic responses of Amangihydrocarbon field using Gassmann fluid substitution

Sonny Inichinbia¹, Peter O. Sule², Aminu L. Ahmed² and Halidu Hamza²

¹Department of Physics, Ahmadu Bello University, Zaria, Nigeria

²Department of Geology, Ahmadu Bello University, Zaria

Abstract: We present a fluid substitution case study of Amangi hydrocarbon field applying Biot-Gassmann theory in which the changes in acoustic parameters (P- and S-wave velocities and density) were modelled. Shear wave velocity was predicted using Greenberg and Castagna empirical relationships between P-wave and S-wave velocities. The results of fluid substitution compare favorably to the available sidewall data. The amplitude character of seismic reflections varied with offset, due to changes in the angle of incidence. The wells on the field penetrated several stacked channelized shoreface sands of variable qualities at depths of 2,702 m and 2,919 m and with thicknesses of 89.05 m and 25.67 m respectively. Well-002 underwent fluid substitution, using the basic Gassmann's theory, with brine and gas assumptions. During fluid substitution, it was assumed that porous rock contains only one type of solid with a homogeneous mineral modulus and the pore space is statistically isotropic. The Lamé parameters were calculated for the two fluid states. The wet case assumed 100% water saturation and brine salinity of 8,000 ppm. The gas case assumed 80% gas saturation. The reservoir sand quality was determined by shale percentage less than 0.4 and porosity greater than 20%. The gas gravity was 0.68.

Keywords: Fluid substitution, hard sand, insitu and brine synthetics, reflectivity, elastic properties, sonics

I. Introduction

The mechanics of fluid substitution is an important part of the seismic rock physics analysis which provides a tool for fluid identification and quantification in reservoir using Gassmann's equation. Amangi field was covered by a recent anisotropic 3D seismic data that was acquired between 2008 and 2010 and processed in 2011. Some more appraisal wells have also been drilled in this area and logging activities carried out in them. There are challenges in the data set of the field, which include the distribution of reservoir properties such as porosity, net pay thickness, fluid type and fluid saturation, as well as the discrimination of hydrocarbon bearing sands from shales, and more importantly, the separation of gas sands from brine saturated sandstones.

Therefore, fluid substitution on well log data was performed using the Gassmann's model. The equations and software implementations (RokDoc version 5.3.4.) are straightforward and the input parameters were quality controlled. To estimate the effect of the pore fluid on the elastic properties, the Gassmann fluid substitution approach was used to model different scenarios and to make reliable estimates of V_p , V_s and density ρ , porosity and also get an indication of the sensitivity of the seismic response to the presence of gas or brine in the reservoir rock.

The objective of this Gassmann fluid substitution is to model the seismic properties (seismic velocities: V_p , V_s) and density ρ , of the two reservoirs (H1000 and H4000) at given reservoir conditions (e.g., pressure, temperature, porosity, mineral type and water salinity) and pore fluid saturation such as 80% - 100% water saturation and hydrocarbon with only gas saturation. This was performed on well log data using Gassmann's equations to analyze the sensitivity of each fluid indicator to model the changes of these parameters at given conditions.

Traditional AVO and petrophysical analysis extract and exploit anomalous variations between seismic compressional wave velocities (V_p) and shear wave velocity (V_s) to indicate changes primarily in pore fluid as well as lithology [1]. The underlying emphasis on seismic wave velocity and density arises from the Knott-Zoeppritz equations for continuity of displacement and stress across an interface between different rock properties for a propagating seismic wave.

A key problem in rock physics well log analysis is the prediction of seismic velocities of rocks saturated with one fluid from measurements on the same rocks saturated with another fluid. The standard method used for performing such fluid substitutions is the approach based on the theory of Gassmann. The Gassmann theory assumes that the pore space is connected and that the pore fluid can flow freely throughout the rock volume sufficiently fast to instantaneously equilibrate the seismically induced pore pressures. Gassmann fluid substitution allows well logs recorded over an interval with one fluid to be modified so as to have the properties of logs recorded over the same interval but with a different insitu fluid(s).

Fluid substitutions are an important part of any seismic attribute study, as they provide the interpreter with a valuable tool for modelling various fluid scenarios which might explain an observed AVO anomaly. Modelling the effect of fluid saturation in reservoir rocks is essential for hydrocarbon reservoir characterization. Fluid substitution is the process by which new acoustic parameters (i.e., moduli, densities, and velocities) are theoretically calculated when the pore fluids are changed from a known saturation to a new saturation. Such a need arises during seismic modelling and AVO analysis. The equations generally used are those from Gassmann and Biot. The combined formulation is the Biot-Gassmann theory[2].

Gassmann fluid substitution is an essential tool of an amplitude analysis workbench. The AVO effect represents a potentially powerful tool to discriminate between brine and hydrocarbon saturated reservoirs. Brine filled reservoirs often show variations in amplitude with offset that are different from those of hydrocarbon filled reservoirs. However, it means going back to the prestack domain. Studying the prestack differences in detail can indicate the causes of near and far offset amplitude variability. The seismic signature from a gas sand is different from the brine filled response when the same reservoir is observed under similar conditions. In such a situation, the encasing geology is probably the same and has little influence on the observed anomalous amplitude behaviour. A distinct change in zero offset reflectivity is probably the most remarkable phenomenon. Changes in amplitude with offset can occur in hydrocarbon as well as brine bearing reservoirs; in that case the intercept might contain the vital pore fill information[3].

II. Field location and geology

Amangi Field measures about 12 km x 5 km and is located 70 km northwest of Port Harcourt within the northeastern corner of licence OML 21 and extends into the adjacent licence OML 53 as shown in Fig. 1. The Field is in the Greater Ughellidepobelt of the Niger Delta, which is in the Gulf of Guinea on the west coast of Central Africa. Niger Delta is in the southern part of Nigeria between latitudes 4° N and 6° N and longitudes 3° E and 9° E. It is bounded in the south by the Gulf of Guinea and in the north by older (Cretaceous) tectonic elements which include the Anambra Basin, the Abakaliki uplift, and the Afikpo syncline.).

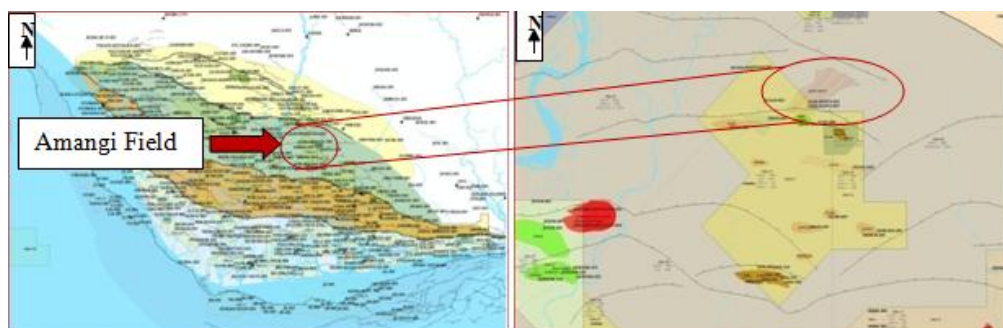


Figure 1. Map of the Niger Delta of Nigeria showing the location of the area of study.

It is bounded to the north and south by large listric normal faults associated with gravity collapse in the Delta. The Tertiary age siliciclastic deposits forming the Niger Delta are attributed to three different lithostratigraphic formations: the Akata Formation, the Agbada Formation, and the Benin Formation. The Agbada Formation (Paralic Cycles) makes up the majority of the oil and gas reservoirs of the Niger Delta including Amangi field, and comprises alternating sandstone/shale bedsets interpreted to represent the delta front, distributary channels and the deltaic plain. The upper part has higher sandstone content than the lower part, demonstrating the progressive seaward advance of the Niger delta through geological time.

III. Well log data

The location of the wells in the field is displayed in Fig. 2. A total of four wells are sited in OML 21 while only two wells are sited in OML 53. Extensive logging dataset were acquired and displayed in Table 1.

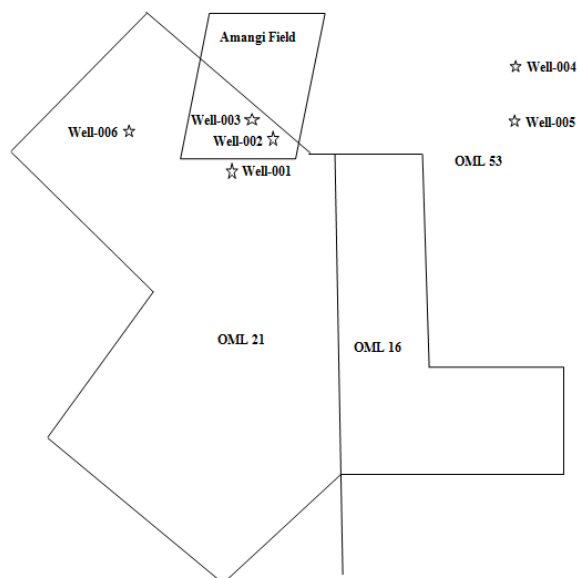


Figure 2. OML map of the study area showing the locations of the wells used in this study. Four out of a total of six wells are located in OML 21 whereas the rest two wells are sited in OML 53.

Table 1. Some wells in Amangi Field showing suite of logs in each well. Only well-002 has a complete suite of good quality logs in the area, needed for this work.

Well	GR (API)	CALL. (inches)	RESIS. (Ω m)	DEN. (g/cm^3)	SONIC ($\mu s/ft$)	PRES. (psi)	FIT	Checkshot(ms)
Well-001	YES	YES	YES	NO	YES	NO	NO	YES
Well-002	YES	YES	YES	YES	YES	YES	YES	YES
Well-003	YES	YES	YES	YES	YES	YES	NO	NO
Well-004	YES	YES	YES	YES	YES	NO	NO	NO
Well-005	YES	YES	YES	YES	YES	NO	NO	NO

From the table well-002 was identified with a complete suite of good quality logs that sampled all or most of the logging types and lithologies and some of its logs are further displayed in Fig. 3. The sonic data were calibrated with the checkshot data. The lithology classification is shown in track 7 in which sand is yellow and shale is green. Compressional and shear sonic logs in (tracks 3 and 4) and density log is in track 14. Resistivity and porosity curves are in tracks 6 and 11, respectively. The gamma ray, calliper, neutron, neutron-density, V_p , and V_s curves are in tracks 2, 5, 8, 9, 10, 12 and 13 respectively. The measured depth and the two way travel time are recorded in track 1. The numbering of the tracks is done from left to right. The calliper log shows stable borehole conditions.

In sand dominant sections, borehole quality is relatively good. The hydrocarbon sand sections have distinct log motifs and properties as compared to the underlying and overlying shale. The thick gas reservoirs are characterized by higher resistivities and neutron-density crossover. The reservoir sands are recognized by their very low gamma ray, low density, low sonic, very high resistivity, and high neutron-porosity. The sands are siliciclastic, finegrained, soft to moderately hard, showing fining upward motifs and sometimes blocky, coarsening upward motifs. Sandstone layers are separated by shale. Sidewall samples, checkshot and vertical seismic profiling (VSP) data were available for this study.

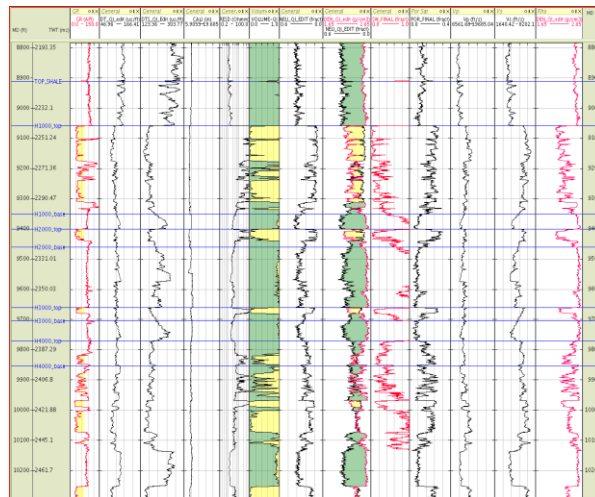


Figure 3. Typical log signatures of shales/sands section in the area of study as seen in well-002. Gamma ray, sonic, caliper, resistivity, volume shale, neutron, porosity, water saturation, V_p , V_s and density logs from well-002 used in this study. The thick gas reservoirs are characterized by higher resistivities and neutron-density crossover.

IV. Sequence stratigraphy and regional correlation of Amangi Field

Amangi field sediments comprise a series of sand and shale successions that have been deposited during different relative sea level changes. These sediments have characteristic coarsening upward, fining upward, blocky and serrated gamma ray/self potential log profiles. Some sands are deposited within the thick shale package and are dominated by incised progradational shoreface deposits. Some sections of the sand are thicker and comprised of more stacked channel sand deposits with some estuarine influences and tidal channel deposits. Below both sands there is another thick shale package. A subregional correlation was made between some of the wells in the study area and is displayed in Fig. 4. The H1000 sands of well-002 maintain a similar log profile to other wells which are located 7 km south of the field. Sands and shales thicken to the north (well-001 to well-006) due to synsedimentary activity on the growth fault at the north of the field. Sediment influx from the north to the southern part of the field.

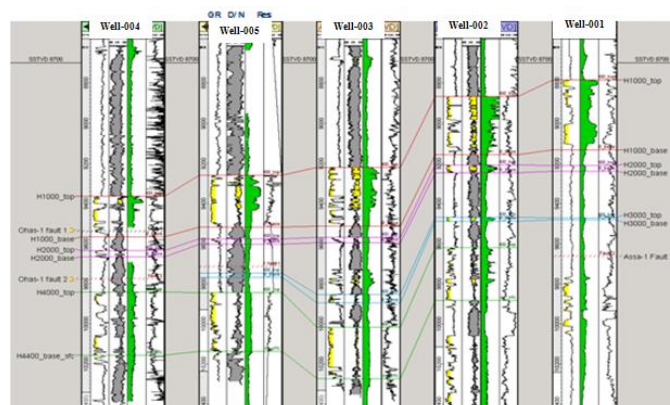


Figure 4. Panel showing a subregional correlation of wells in the area of study

V. Methodology

A key step in our interpretation of AVO first entailed modelling the expected responses for the various lithologies and fluids that produce amplitude anomalies. To do this we utilized a well (well-002) that penetrated a known seismic anomaly and where a dipole sonic had been run, yielding both P-wave and S-wave data. After conducting the AVO analysis for the actual well data, we then removed and substituted insitu fluids and modelled the results.

The common-mid-point (CMP) gather after flattening illustrated the variation for different traces. It was ensured that the data on the individual CMP gathers come from a consistent subsurface location. This was achieved by migration of the input data set and careful data preconditioning. The synthetics were calculated along a normal incidence and zero offset trajectory and the hydrocarbon saturation was set at 80%. The seismic

velocities of an isotropic rock material can be estimated using known rock moduli K and density ρ . P- and S-wave velocities in isotropic media are estimated below:

$$V_p = \sqrt{\frac{K + \frac{4}{3}\mu}{\rho}} \dots\dots\dots (1)$$

$$V_s = \sqrt{\frac{\mu}{\rho}} \dots\dots\dots (2)$$

Respectively, where V_p and V_s are the P-wave and S-wave velocities, K and μ are the bulk and shear moduli, and ρ is the mass density. The Gassmann's equations relate the bulk modulus of a rock to its pore, frame and fluid properties. The bulk modulus of a saturated rock is given by the low frequency Gassmann theory:

$$K_{sat} = K_{dry} + \frac{\left(1 - \frac{K_{dry}}{K_{matrix}}\right)^2}{\frac{\phi}{K_{fluid}} + \frac{1-\phi}{K_{matrix}} - \frac{K_{dry}}{K_{matrix}^2}} \dots\dots\dots (3)$$

where K_{sat} , K_{dry} , K_{matrix} and K_{fluid} are the bulk moduli of the saturated rock, porous rock frame (dry or drained of any pore filling fluid), mineral matrix and pore fluid respectively, and ϕ is porosity (as fraction). In the Gassmann formulation shear modulus is independent of the pore fluid and held constant during the fluid substitution. Bulk modulus (K_{sat}) and shear modulus (μ) at in-situ or initial condition was estimated from the wireline log data (seismic velocities and density) by rewriting the P- and S- wave velocities equations in isotropic media. Thus:

$$K_{sat} = \rho \left(V_p^2 - \frac{4}{3} V_s^2 \right) \dots\dots\dots (4)$$

$$\mu = \rho V_s^2 \dots\dots\dots (5)$$

where V_p and V_s are the P- and S- wave velocities, K and μ are the bulk and shear moduli and ρ is the matrix density [4].

To estimate the saturated bulk modulus (6), at a given reservoir condition and fluid type we estimated dry or frame bulk modulus, matrix and pore fluid as follows:

$$K_{dry} = K_{sat} \frac{\left(\frac{\phi K_{matrix}}{K_{fluid}} + 1 - \phi \right) - K_{matrix}}{\frac{\phi K_{matrix}}{K_{fluid}} + \frac{K_{sat}}{K_{matrix}} - 1 - \phi} \dots\dots\dots (6)$$

Where the symbols retained their usual meanings as stated in (3). Then with known K_{dry} , we can estimate V_p and V_s when the pore fluid changes and various hydrocarbon indicators can be estimated [5].

To calculate the bulk modulus of mineral matrix, we need to know the mineral composition of rock from the laboratory examination of core samples. But in the absence of core data, as was the case of this research work, lithology was assumed to be a composition of quartz and clay minerals. The clay percentage was derived from the volume shale (V_{sh}) curve derived from the gamma ray log. Typically, shale contains about 70% clay 30% of other minerals -mostly quartz. Having determined the abundances, K_{matrix} was calculated by the application of Voigt-Reuss-Hill averaging of the mineral constituents. Inputs were V_{sh} , bulk modulus of clay K_{clay} and bulk modulus of quartz K_{quartz} . But $V_{quartz} = 1 - V_{clay}$ and $V_{clay} = 70\% V_{sh}$ (assumption). Where V_{clay} means volume of clay and V_{quartz} means volume of quartz. Similarly, density of the mineral matrix ρ_{matrix} . Bulk modulus and density of gas in a reservoir depend on the pressure, temperature and the type of gas [4].

The mechanics of fluid substitution on the density, compressional and shear logs is simple. For the density log, fluid substitution can be written as:

$$\rho_{b2} = \rho_{b1} - (\phi \rho_{f1} - \phi \rho_{f2}) \dots\dots\dots (7)$$

Where ρ_{b1} is the initial rock bulk density, ρ_{b2} is the bulk rock density after fluid substitution, ρ_{f1} is the initial fluid density, ρ_{f2} is the density of the substituting fluid and ϕ is the porosity. The substituted rock density ρ_{b2} is simply

the fractional difference attributable to the fluid change in the pore space. This equation describes the relationship between the fluid density, porosity, grain density of the rock matrix, and the rock bulk density and is also easily rewritten and solved for porosity [6].

Given the fact that in Gassmann's model the shear modulus is independent of the pore fill, the substituted V_s depends only on the change in density:

$$V_{s2} = \sqrt{\frac{\mu}{\rho_{b2}}} \dots\dots\dots (8)$$

This means that substitution of hydrocarbon for water/brine will result in a lowering of bulk density and an increase in V_s .

Calculating the fluid substitution effect on the compressional wave velocity V_p , as measured by the sonic log, is not so straightforward because it depends not only on the substituted density and the shear modulus, but also on the saturated bulk modulus K_{sat} :

$$V_{p2} = \sqrt{\frac{K_{sat2} + \frac{4}{3}\mu}{\rho_{b2}}} \dots\dots\dots (9)$$

In turn the bulk modulus of the new rock requires knowledge of the mineral modulus K_o , the fluid modulus K_f and the pore space stiffness K_ϕ :

$$K_{sat2} = \frac{1}{\frac{1}{K_o} + \frac{\phi}{K_\phi + \frac{K_o K_{f2}}{K_o - K_{f2}}}} \dots\dots\dots (10)$$

$$K_\phi = \frac{\phi}{\frac{1}{K_{sat1}} - \frac{1}{K_o}} - \frac{1}{\frac{1}{K_{f1}} - \frac{1}{K_o}} \dots\dots\dots (11)$$

The pore space stiffness K_ϕ is related to porosity, mineral modulus and the dry rock bulk modulus K_d by:

$$K_\phi = \frac{\phi}{\frac{1}{K_d} - \frac{1}{K_o}} \dots\dots\dots (12)$$

Having these various parameter relationships, two particular effects are important in determining the magnitude of the fluid substitution effect on the velocity log. These relate to the role of pore stiffness and the effect of gas saturation.

The second important aspect of fluid substitution is the effect of gas saturation. Generating a value for the fluid bulk modulus to input into Gassmann requires that the bulk modulus of water/brine K_w and hydrocarbon K_h are mixed according to the water saturation S_w in the pore space. For seismic applications the fluid bulk modulus is usually calculated using the Reuss average:

$$\frac{1}{K_f} = \frac{S_w}{K_w} + \frac{1-S_w}{K_h} \dots\dots\dots (13)$$

Using this mixing law for substituting gas into a rock often leads to the type of $S_w - V_p$ relationship that shows that a small amount of gas has a large effect on the rock bulk modulus, producing a dramatic decrease in V_p . With increasing gas the significant change is in the density rather than the bulk modulus, such that following (9), V_p increases with increasing gas saturation [5]. Thus, the importance of the influence of reservoir fluids on the elasticity of rocks has long been recognized and used by well logging specialists in formation evaluation work.

Fig.5 illustrates changes in seismic response when the gas saturated reservoirs were replaced by brine. The synthetics were calculated along a normal incidence and zero offset trajectory. The gas saturation was set at 80%. The brine case shows brightening of the reflection with respect to the gas filled scenario because the H1000 sand has higher P-impedance than the encasing shales and is hard sand displaying increased amplitude and reversal of phase at the top of the reservoir sands. Both the H1000 and H400 reservoirs showed this increased contrast tendency, because both sands have higher P-impedance than the encasing shales. There is a decrease in V_p , V_s and density indicating the presence of gas and porosity of the reservoir.

In Fig.5, sets of well logs were produced representing the gas and brine cases. A model, based on these logs, was produced at seismic resolution, from the surface to the base of the logs. The models were ray traced in order to understand the angle of incidence / offset relationship at each interface. Finally a modified form of the Zoeppritz equations given by Aki and Richards was used to calculate the reflection coefficients at the interfaces/offset locations. These “spike” gathers were then convolved with a wavelet to produce synthetic gathers at normal incidence, one for the insitu (gas) case, the other for the brine case.

Firstly, we decided to demonstrate the effect of the fluid substitution on the seismic response using the near offset because of the fact that if the gas were replaced by brine in the same reservoir units, the main change would occur in the zero offset $R(0)$ reflectivity, while the amplitude gradient is not necessarily affected as much. The change in zero offset reflectivity $R(0)$, or intercept, is the most diagnostic feature. The fluid substitution effect on the seismic response is illustrated on the two reservoirs H1000 and H4000. We observe that not only the top of the reservoirs’ reflections changes but also the reflections below the reservoirs. The top of the reservoir H1000 corresponds to a trough on the synthetic trace while that of H4000 corresponds to a peak. The reservoir sands have equal P-impedance as the overlying shales.

Fig. 5 illustrates changes in seismic response when the gas saturated reservoirs were replaced by brine. The synthetics are calculated along a normal incidence and zero offset trajectory. The gas saturation is set at 80%. The brine case shows brightening of the reflection with respect to the gas filled scenario because the H1000 sand has higher P-impedance than the encasing shales and is “hard” sand displaying increased amplitude and reversal of phase at the top of the reservoir sands. Both the H1000 and H4000 reservoirs showed this increased contrast tendency, because both sands have higher P-impedance than the encasing shales. There is a decrease in V_p , and density indicating the presence of gas and increased porosity of the reservoir.

Fluid substitution to brine makes H1000 sand harder than insitu condition as we can observe from the trough amplitudes of the brine synthetics. The magnitudes of the trough amplitudes of the brine synthetics at the top of the H1000 sand are larger than the amplitudes of the insitu synthetics on the same horizon. Fluid substitution to brine makes H4000 sand softer than insitu synthetics as displayed by the peak amplitudes of the top of the H4000 sand. The magnitudes of the peak amplitudes of the brine synthetics of the top of the H4000 sand are smaller than the magnitudes of the peak amplitudes of the insitu synthetics of the top of the H4000.

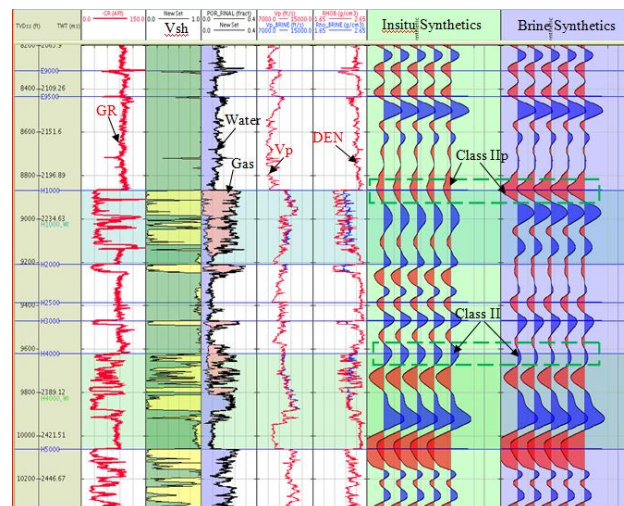


Figure 5. Gassmann’s fluid substitution and synthetics generation at normal incidence, modeling seismic responses at the reservoirs tops. Fluid substitution to brine makes H1000 harder than insitu condition and Fluid substitution to brine makes H4000 softer than insitu condition.

Similarly, Gassmann fluid substitution at oblique angle of incidence modelled the seismic response of the shear wave as shown in Fig.6. The elastic approach takes into account the behaviour of both V_p and V_s . It provides better discrimination of the effects caused by the changes in pore fill, and the AVO behaviour is more accurately modelled. The assumption is made that V_p is approximately twice V_s and the higher terms are dropped under the 30° angle of incidence condition. The well logs and the objective (marker zone) are presented in Fig.5 with the insitu properties displayed in green and the fluid replacement logs displayed in blue. Strong increases in V_p , V_s and bulk density are observed in the fluid replacement logs, which are typical for high acoustic impedance bright spots in unconsolidated Tertiary strata.

This section in addition models the V_s response to fluid substitution to brine. We replaced the insitu gas with brine and the inferred fluid properties are included in Fig.6. Large differences are observed in the density and compressional velocity response between gas and brine, whereas much smaller differences are observed in

shear velocity. There is a decrease in V_p , V_s and density indicating the presence of gas and the porosity of the reservoir. Note, that the V_s for gas are faster than that for brine.

The essence of AVO analysis lies in the fact that the shear modulus of a rock does not change when the fluid saturant is changed. However, the bulk modulus changes significantly when the fluid saturant is changed. The bulk modulus of a brine saturated rock is greater than that of gas saturated rock brine being significantly stiffer than gas. These elastic constants are linked to seismic velocity, as shown in the above relations and result in the V_p of a gas saturated rock being significantly less than the V_p for the same rock if it were brine saturated. The V_s of a gas saturated rock is slightly higher than V_s for the same rock if it were brine saturated, the density of gas being lower than the density of brine. The V_p/V_s ratio of gas saturated rock can thus be substantially different from the V_p/V_s ratio for the same rock if it were brine saturated.

Thus, forward modelling was performed to observe the AVO response of the sands (Figs.5 and 6). At normal incidence, reflectivity is quite low due to the low impedance contrast between the sand and shale. The amplitude at the interface is negative and increases with increasing angle. Therefore, the change in lithology from shale to sand results in an observable variation of the seismic amplitude with offset. Based on these modelling results, it was decided to invert for V_p and V_s using the prestack data to generate a V_p/V_s volume that could distinguish the sands from the shale within the zones of interest.

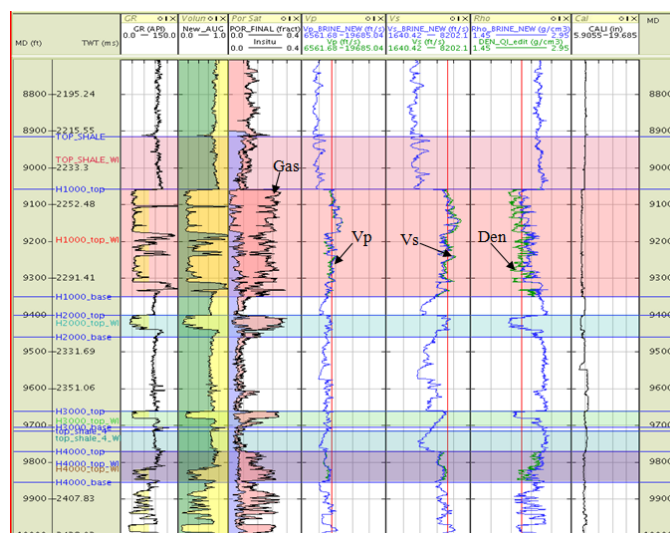


Figure 6. Gassmann's fluid substitution and synthetics generation at oblique angle of incidence, modelling seismic responses at the reservoirs intervals. Fluid substitution to brine makes H1000 harder than insitu condition and fluid substitution to brine makes H4000 softer than insitu condition. Fluid substitution was carried out to get an indication of the sensitivity of the seismic response to the presence of gas or water in the reservoir rocks.

The fluid substitution showed that log values in the gas zone were actually very close to the Gassmann estimated brine saturated values. Realistic reservoir fluid properties (gas-oil ratio: its a gas reservoir; gas gravity 0.65, gas density 0.808 g/cm³, brine density 0.859 g/cm³, temperature 210 F, pressure 6050 Psi, salinity 8000ppm for the H1000 reservoir and gas density, 0.804 gm/cm³, brine density 0.825 g/cm³, temperature 220 F, pressure 6150 psi, salinity 8000ppm for the H4000 reservoir) were used in the fluid substitution calculation using Gassmann's equations. We could see the separation more in density, then in the shear wave and least in the P-wave in line with theory.

Note the introduction of even a small amount of hydrocarbon into a brine filled reservoir results in a large decrease in P-wave velocity, but density and V_s change only slightly. When a reservoir is fully charged with hydrocarbons, the density drops and the shear velocity increases compared with the brine filled values. Thus, Gassmann's equations provide the seismic interpreter with a powerful framework for evaluating various fluid scenarios which might give rise to an observed seismic anomaly.

Indeed, seismic inversion provides a perception of some of the rock parameters, but the separate contributions of velocity and density are still difficult to substantiate. This knowledge will ultimately result in a better lateral prediction of the reservoir behaviour. It should be kept in mind that most of the time more than one solution exists for a given inversion problem. In view of this, other criteria have to be examined with regard to their usefulness in putting constraints on the number of solutions [3]. Analysis of crossplot clustering and also multiattribute analysis are employed in this study because they are promising techniques in this respect.

Plots of P-wave reflectivity versus incidence angle (θ) from well log data are shown in Fig.7 for both reservoirs and we discovered from analysis that these reservoirs produce typical Class II AVO response. The H1000 sand shows Class IIp AVO response with phase reversal, whereas H4000 sand shows a Class II response without phase reversal for the angle ranges displayed. H1000 sand has a highvelocity than the overlying shale so it is “hard” sand. This was as a result of mixedlithologies (heterolithics) as evident in the sidewall samples available for this study.

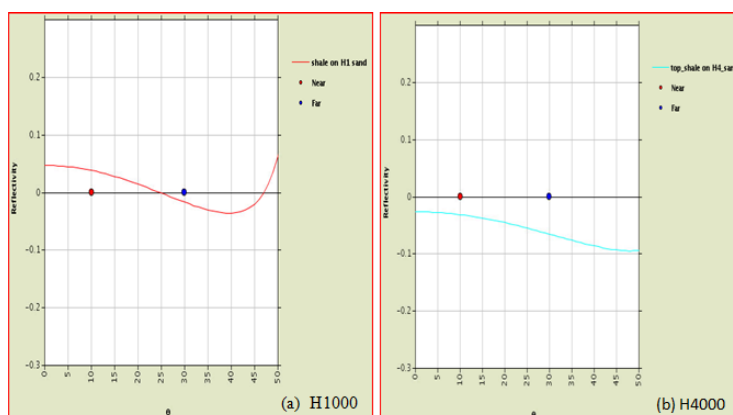


Figure 7. AVO classes of the reservoirs. (a) Class IIp AVO response at top of H1000 sand and (b) Class II AVO response at top of H4000 sand.

VI. Conclusion

The importance of accurate estimates of seismic velocities, both V_p and V_s , and to understand effects of fluid properties on seismic velocities in well logging, seismic interpretation, reservoir monitoring, and so on cannot be overemphasized. The influence of saturation by water, gas and mixtures of these fluids on the densities, velocities, reflection coefficients, and elastic moduli of rocks under different environments were determined to aid in formation evaluation.

The method was applied via industry proprietary software packages with knowledge of the calculations and pitfalls critical for generating consistent and meaningful results. We are able to obtain reliable models of V_p , V_s and ρ to quantify the differences between the hydrocarbon and brine case by crossplot analysis, interface modelling and offset synthetic analysis. This work provided the seismic interpreters with a powerful framework for evaluating various fluid scenarios which gave rise to the observed seismic anomalies.

The Gassmann fluid substitution applied to this field has increased the understanding of the observed seismic response which ultimately led to a better lateral prediction of reservoir properties with delineation of the sweetspots and this could also lead to improved volumetric prognosis. This will result in better reservoir management decisions, with augmented recovery factors and an improved drilling success.

Acknowledgements

The authors are grateful to the Shell Petroleum Development Company of Nigeria Limited for giving us the permission to publish this work. We also appreciate the efforts of Francesca I. Osayande, Prahlad Basak, Lucky M. Omudu, Temitope J. Jegede, Ufuoma Akpomeyoma, Obioma and all those who contributed by way of comments and discussions to make this publication a success. We are indeed grateful to Anthony B. Chokor and the university liaison team of the SPDC.

References

- [1]. B. Goodway, T. Chen and J. Downton, Improved AVO fluid detection and lithology discrimination using Lamé petrophysical parameters: “ $\lambda\rho$ ”, “ $\mu\rho$ ” and “ λ/μ fluid stack”, from P and S inversions, Canadian Society of Exploration Geophysicists Recorder, 1997, 3 – 5.
- [2]. P. N. Mahob, and J. P. Castagna, Fluid substitution and shear-wave velocity prediction including dispersion effects: A case study, NW Shelf, Australia, Society of Exploration Geophysicists, Expanded Abstracts, 2000, 1 – 4.
- [3]. P. Veeken, and R. M. Davies, AVO attribute analysis and seismic reservoir characterization. First Break, 24, 2006, 41 – 52.
- [4]. D. A. Kumar, tutorial on Gassmann fluid substitution: formulation, algorithm and matlab code. GEOHORIZONS, 2006, 4 – 6.
- [5]. R. Simm, Practical Gassmann fluid substitution in sand/shale sequences. First Break, 25, 2007, 61 – 66.
- [6]. T. M. Smith, C. H. Sondergeld and C. S. Rai, Gassmann fluid substitutions: A tutorial. Geophysics, 68(2), 2003, 430 – 440.